PHYSICAL REVIEW D **96,** 046018 (2017)

Baryon number current in holographic noncommutative QCD

Tadahito Nakajima,[1,2] Yukiko Ohtake,[3] and Kenji Suzuki[4]
[1]*Department of Physics, Swansea University, Swansea SA2 8PP, United Kingdom*
[2]*College of Engineering, Nihon University, Fukushima 963-8642, Japan*
[3]*Toyama National College of Technology, Toyama 939-8630, Japan*
[4]*Department of Physics, Ochanomizu University, Tokyo 112-8610, Japan*
(Received 25 February 2017; published 30 August 2017)

We consider the noncommutative deformation of the finite-temperature holographic QCD (Sakai-Sugimoto) model in external electric and magnetic field and evaluate the effect of the noncommutativity on the properties of the conductor-insulator phase transition associated with a baryon number current. Although the noncommutative deformation of the gauge theory does not change the phase structure with respect to the baryon number current, the transition temperature T_c, the transition electric field e_c, and magnetic field b_c in the conductor-insulator phase transition depend on the noncommutativity parameter θ. Namely, the noncommutativity of space coordinates have an influence on the shape of the phase diagram for the conductor-insulator phase transition. On the other hand, the allowed range of the noncommutativity parameter can be restricted by the reality condition of the constants of motion.

DOI: 10.1103/PhysRevD.96.046018

I. INTRODUCTION

Noncommutative gauge theories (gauge theories on noncommutative Moyal space) can be realized as low-energy theories of D branes with the Neveu-Schwarz–Neveu-Schwarz (NS-NS) B (two-form) field [1–7]. The noncommutativity of space coordinates brings nontrivial properties on the gauge field theory at the quantum level. A remarkable phenomenon is the so-called UV/IR mixing [8], where the UV and IR degrees of freedom of the theory are mixed in a complicated nontrivial way. Although the noncommutative gauge theories have been studied extensively, it is hard to investigate them in the perturbative approach. Little is currently known of the nonperturbative properties of noncommutative gauge theories.

The noncommutative Yang-Mills theories have gravity duals of which the near-horizon region describes the noncommutative Yang-Mills theories in the limit of large N_c and large coupling [9–11]. Based on the generalized gauge/gravity (or AdS/CFT) duality, we can explore the nonperturbative aspects of the noncommutative gauge theories. For instance, the noncommutativity of space coordinates modifies the Wilson loop behavior [12–14] and glueball mass spectra [15]. The gravity duals of noncommutative gauge theories with matter in the fundamental representation have also been constructed by adding probe flavor branes [16]. Employing the gravity dual description of noncommutative gauge theories with flavor degrees of freedom, we have been able to find that the noncommutativity is also reflected in the flavor dynamics. For instance, the mass spectrum of mesons can be modified by the [16].

Fundamental properties of QCD at low energies are confinement and chiral symmetry breaking. The Sakai-Sugimoto model (a holographic QCD model with the D4-D8-$\overline{\text{D8}}$-brane system) has been known to capture these properties of QCD at low energies [17,18]. The holographic QCD models can be modified to introduce finite temperature. The phase of chiral symmetry breaking and restoration can be interpreted as configurations of probe branes in this model [19–21]. The effect of the noncommutativity on the chiral phase transition has been examined by the noncommutative deformation of the holographic QCD model at finite temperature. The phase diagrams for the chiral phase transition can be deformed by the noncommutativity of space coordinates [22].

It has been shown that the large N_c QCD at finite temperature has a conductor and insulator phase associated with a baryon number current within a framework of the finite-temperature Sakai-Sugimoto model in the external electric and magnetic field [23,24], *à la* Karch-O'Bannon [25]. This conductor-insulator phase transition is closely related to the chiral phase transition in the finite-temperature Sakai-Sugimoto model. This fact suggests the possibility that the phase diagrams for the conductor-insulator phase transition associated with a baryon number current can also be deformed by the noncommutativity of space coordinates.

We construct the noncommutative deformation of the finite-temperature holographic QCD (Sakai-Sugimoto) model in the external electric and magnetic field and evaluate the effect of the noncommutativity on the properties of the conductor-insulator phase transition associated with a baryon number current. As will be seen later, the baryon number current, the conductivity, and the phase diagrams for the conductor-insulator phase transition can

be deformed by the noncommutativity of space coordinates.[1] The Wess-Zumino term in the effective action of the probe branes plays the role of the noncommutative deformation on the properties of the conductor-insulator phase transition.

This paper is organized as follows. In Sec. II, we introduce the holographic QCD (Sakai-Sugimoto) model at finite temperature and discuss the features of the phase transition. Then, we construct the noncommutative deformation of this model. In Sec. III, we investigate the response of the baryon number current to the external electric field and evaluate the noncommutative deformation of the baryon number current, the conductivity, and the phase diagrams for the conductor-insulator phase transition. In Sec. IV, we investigate the response to the external magnetic field and evaluate the noncommutative deformation of the phase diagrams. Section V is devoted to conclusions and discussions.

II. NONCOMMUTATIVE DEFORMATION OF THE HOLOGRAPHIC QCD MODEL AT FINITE TEMPERATURE

In this section, we consider a noncommutative deformation of the holographic QCD (Sakai-Sugimoto) model at finite temperature based on the prescription of Ref. [16]. The holographic QCD model is a gravity dual for a $4+1$-dimensional QCD with $\mathrm{U}(\mathrm{N}_f)_L \times \mathrm{U}(\mathrm{N}_f)_R$ global chiral symmetry of which the symmetry is spontaneously broken [17,18]. This model is a D4-D8-$\overline{\mathrm{D8}}$-brane system consisting of S^1 compactified N_c D4 branes and N_f D8-$\overline{\mathrm{D8}}$ branes pairs transverse to the S^1. The near-horizon limit of the set of the N_c D4 branes solution compactified on S^1 takes the form,

$$\begin{aligned} ds^2 &= \left(\frac{u}{R_{\mathrm{D4}}}\right)^{3/2}(-(dt)^2+(dx^1)^2+(dx^2)^2+(dx^3)^2 \\ &\quad + f_K(u)d\tau^2) + \left(\frac{R_{\mathrm{D4}}}{u}\right)^{3/2}\left(\frac{du^2}{f_K(u)}+u^2 d\Omega_4^2\right), \\ R_{\mathrm{D4}}^3 &= \pi g_s N_c l_s^3, \qquad f_K(u) = 1-\frac{{u_K}^3}{u^3}, \end{aligned} \tag{2.1}$$

where u_K is a parameter; u is the radial direction bounded from below by $u \geq u_K$; τ is the compactified direction of the D4-brane world volume which is transverse to the D8-$\overline{\mathrm{D8}}$ branes; and g_s and l_s are the string coupling and the string length, respectively. The dilaton ϕ and the field strength F_4 of the RR 3-form C_3 are given by

[1]The noncommutative deformation on the conductivity associated with a baryon number current has been examined by Ref. [26]. The response of the properties of the conductor-insulator phase transition associated with a baryon number current to the NS-NS field has been examined by Ref. [27].

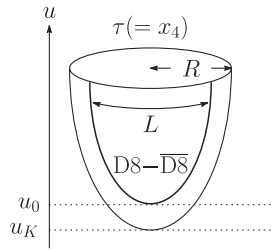

FIG. 1. The D8-$\overline{\mathrm{D8}}$ branes configurations at low temperature.

$$e^{\phi} = g_s\left(\frac{u}{R_{\mathrm{D4}}}\right)^{3/4}, \qquad F_4 = dC_3 = \frac{2\pi N_c}{V_4}\epsilon_4, \tag{2.2}$$

where $V_4 = 8\pi^2/3$ is the volume of unit S^4 and ϵ_4 is the corresponding volume form. To avoid a conical singularity at $u = u_K$, the τ direction should have a period of

$$\delta\tau = \frac{4\pi}{3}\left(\frac{R_{\mathrm{D4}}^3}{u_K}\right)^{1/2} = 2\pi R = \frac{2\pi}{M_{\mathrm{KK}}}, \tag{2.3}$$

where R is the radius of S^1 and M_{KK} is the Kaluza-Klein mass. The parameter u_{K} is related to the Kaluza-Klein mass M_{KK} via the relation (2.3). The five-dimensional gauge coupling is expressed in terms of g_s and l_s as $g_{\mathrm{YM}}^2 = (2\pi)^2 g_s l_s$. The gravity description is valid for strong coupling $\lambda \gg R$, where as usual $\lambda = g_{\mathrm{YM}}^2 N_c$ denotes the 't Hooft coupling.

Next, we consider the probe D8 branes and anti-D8-branes ($\overline{\mathrm{D8}}$-branes) which span the coordinates $t, x^i (i = 1,2,3), \Omega_4$. They are treated as probes in the D4-brane background. The flavor degrees of freedom are introduced by strings stretching between the D4 branes and D8 ($\overline{\mathrm{D8}}$) branes. The D8 branes and $\overline{\mathrm{D8}}$ branes are connected at $u = u_0$ as shown in Fig. 1. The connected configuration of the D8-$\overline{\mathrm{D8}}$ branes indicates that the $\mathrm{U}(\mathrm{N}_f)_L \times \mathrm{U}(\mathrm{N}_f)_R$ global chiral symmetry is broken to a diagonal subgroup $\mathrm{U}(\mathrm{N}_f)$. We refer to the connected configuration in the low temperature as the low-temperature phase.

The holographic QCD model at finite temperature has been proposed in Refs. [19–21]. To introduce a finite temperature T in the model, we consider the Euclidean gravitational solution, which asymptotically equals (2.1) but with the compactification of the Euclidean time direction t_E. In this solution, the periodicity of t_E is arbitrary and equals $\beta = 1/T$. Another solution with the same asymptotic is given by interchanging the role of t_E and τ directions,

$$\begin{aligned} ds^2 &= \left(\frac{u}{R_{\mathrm{D4}}}\right)^{3/2}(f_T(u)(dt_E)^2+(dx^1)^2+(dx^2)^2 \\ &\quad + (dx^3)^2+d\tau^2) + \left(\frac{R_{\mathrm{D4}}}{u}\right)^{3/2}\left(\frac{du^2}{f_T(u)}+u^2 d\Omega_4^2\right), \\ R_{\mathrm{D4}}^3 &= \pi g_s N_c l_s^3, \qquad f_T(u) = 1-\frac{u_T^3}{u^3}, \end{aligned} \tag{2.4}$$

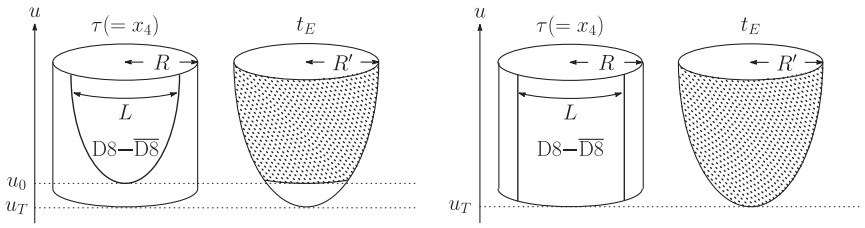

FIG. 2. The D8-$\overline{\text{D8}}$ branes configurations at high temperature.

where u_T is a parameter. The period of the compactified time direction is set to

$$\delta t_E = \frac{4\pi}{3}\left(\frac{R_{\text{D4}}^3}{u_T}\right)^{1/2} = \frac{1}{T} \tag{2.5}$$

to avoid a singularity at $u = u_T$. The parameter u_T is related to the temperature T. The metric (2.1) with the compactification of Euclidean time t_E is dominant in the low temperature $T < 1/2\pi R$, while the metric (2.4) is dominant in the high temperature $T > 1/2\pi R$. The transition between the metric (2.1) and the metric (2.4) occurs at a temperature of $T_d = 1/2\pi R \simeq 0.159/R$. This transition is first order and corresponds to the confinement-deconfinement phase transition in the dual gauge theory side.

In the deconfinement background, there are two kinds of configurations of D8 branes and $\overline{\text{D8}}$ branes as shown in Fig. 2. One is the connected configuration and the other is the disconnected configuration in which the D8 branes and $\overline{\text{D8}}$ branes hang vertically from infinity down to the horizon. The disconnected configuration of the D8-$\overline{\text{D8}}$ branes indicates that the $\text{U}(\text{N}_f)_L \times \text{U}(\text{N}_f)_R$ global chiral symmetry is restored in the dual gauge theory side. The transition between connected-disconnected configuration (chiral phase transition in the dual gauge theory side) is also first order. We refer to the disconnected configuration and the connected configuration in the deconfinement background as parallel embedding of D8 branes and $\overline{\text{D8}}$ branes in the high-temperature phase and U-shaped embedding of D8 branes and $\overline{\text{D8}}$ branes in the intermediate-temperature phase, respectively. The intermediate-temperature phase is realized when the confinement-deconfinement phase transition and the chiral phase transition do not occur simultaneously.

As mentioned above, the classical configuration of D8 branes and $\overline{\text{D8}}$ branes exhibits the flavor physics in the dual gauge theory side. The configuration can be analyzed by the solution of the equation of motion for the D8 branes. Substituting the determinant of the induced metric in the deconfining background and the dilaton into the Dirac-Born-Infeld (DBI) action, we obtain the effective action for the D8 branes,

$$\begin{aligned} S_{\text{DBI}}^{\text{D8}} &= 2N_f T_8 \int d^9x e^{-\phi}\sqrt{\det(g_{MN})} \\ &= \frac{2N_f T_8 V_4}{g_s}\int d^4x du u^4 \sqrt{f_T(u)\tau'(u)^2 + \frac{R_{\text{D4}}^3}{u^3}}, \end{aligned} \tag{2.6}$$

where T_8 is the tension of the D8 brane and the prime of τ denotes differentiation with respect to u. The constant of motion associated with τ, denoted by p, has the form

$$\frac{u^4 f_T(u)\tau'(u)}{\sqrt{f_T(u)\tau'(u)^2 + \frac{R_{\text{D4}}^3}{u^3}}} = p = u_0^4\sqrt{f_T(u_0)}, \tag{2.7}$$

where we assumed that there is a point u_0 that satisfies the condition $\lim_{u\to u_0}\tau'(u) \to \infty$. The solution to the equation of motion for $\tau(u)$ is found to be

$$\tau'(u) = \sqrt{\frac{R_{\text{D4}}^3}{u^3 f_T(u)}}\left[\frac{u^8 f_T(u)}{u_0^8 f_T(u_0)} - 1\right]^{-1/2}, \tag{2.8}$$

by using (2.7). This solution corresponds to the U-shaped embedding of D8 branes and $\overline{\text{D8}}$ branes. There is another solution to the equation of motion for $\tau(u)$ in the deconfinement background. This solution is simply given by $\tau'(u) = 0$ [$\tau(u)$ is a constant] and corresponds to the parallel embedding of D8 branes and $\overline{\text{D8}}$ branes.

The asymptotic D8 branes and $\overline{\text{D8}}$ branes distances can be obtained by integrating (2.8) with respect to u:

$$L = \int d\tau = 2\int_{u_0}^{\infty} du\tau'(u). \tag{2.9}$$

The asymptotic distance L_χ and the temperature T_χ at the chiral symmetry phase transition can be related as $L_\chi T_\chi \simeq 0.154$. For $LT < 0.154$, the U-shaped embedding dominates, and chiral symmetry is broken. On the other hand, for $LT > 0.154$, the parallel embedding dominates, and chiral symmetry is restored. When T_χ is higher than T_d, namely, small $L/R(< 0.97)$, the dual gauge theory is deconfined but with a broken chiral symmetry [19].

The constant of motion p remains a finite value that is given by (2.7) in the U-shaped embedding with a broken chiral symmetry and vanishes in the parallel embedding with a restored chiral symmetry. In this sense, we can regard p as an order parameter for the chiral transition in the deconfined phase. This first-order phase transition behavior can be analyzed from the dependence of the asymptotic distance L on p [23].

The holographic dual description of the noncommutative gauge theories was introduced in Refs. [9–11]. In

accordance with the formulation of Refs. [9–11], we attempt to construct the gravity dual of the noncommutative QCD of which the chiral symmetry is spontaneously broken by deforming the holographic QCD model. Let us consider the D4-branes solution compactified on a circle in the τ direction. T dualizing it along x^3 produces D3 branes delocalized along x^3. After rotating the D3 branes along the (x^2, x^3) plane, we T dualize back on x^3. This procedure yields the solution with B_{23} fields along the x^2 and x^3 directions. The solution in the low temperature takes the form

$$ds^2 = \left(\frac{u}{R_{\rm D4}}\right)^{3/2}((dt_E)^2 + (dx^1)^2 + h\{(dx^2)^2 + (dx^3)^2\} + f_K(u)d\tau^2) + \left(\frac{R_{\rm D4}}{u}\right)^{3/2}\left(\frac{du^2}{f_K(u)} + u^2 d\Omega_4^2\right), \tag{2.10}$$

where $h(u) = \frac{1}{1+\theta^3 u^3}$ and θ denotes the noncommutativity parameter with the dimension of $[\text{length}]^{-1}$. This solution with $\theta \neq 0$ is dual to a gauge theory in which the coordinates x^2 and x^3 do not commute. It is obvious that this solution reduces to the solution (2.1) with the Euclidean signature at $\theta = 0$. In the deconfined phase, the solution (2.4) changes to

$$ds^2 = \left(\frac{u}{R_{\rm D4}}\right)^{3/2}(f_T(u)(dx_E)^2 + (dx^1)^2 + h\{(dx^2)^2 + (dx^3)^2\} + d\tau^2) + \left(\frac{R_{\rm D4}}{u}\right)^{3/2}\left(\frac{du^2}{f_T(u)} + u^2 d\Omega_4^2\right). \tag{2.11}$$

The solution has the same form as the one in the confined phase (2.10), but with the roles of the τ and t_E directions exchanged.

The effective action of probe D8 branes is given by the DBI action with the Wess-Zumino (WZ) term,

$$\begin{aligned} S^{\rm D8} &= S^{\rm D8}_{\rm DBI} + S^{\rm D8}_{\rm WZ}, \\ S^{\rm D8}_{\rm DBI} &= T_8 \int d^9x e^{-\phi} {\rm Tr}\sqrt{\det(g_{MN} + B_{MN} + 2\pi\alpha' F_{MN})}, \\ S^{\rm D8}_{\rm WZ} &= \mu_8 \int_{\rm D8} C_3 \wedge e^{(\tilde{B} + 2\pi l_s{}^2 F)}, \end{aligned} \tag{2.12}$$

where μ_8 is the D8-brane charge. The dilaton field ϕ and the antisymmetric tensor field $\tilde{B} = B_{MN}dx^M dx^N$ have the following form:

$$e^{2\phi} = g_s{}^2 h(u)\left(\frac{u}{R_{\rm D4}}\right)^{3/2}, \tag{2.13}$$

$$B_{MN}(u) = \begin{cases} \theta^{3/2}\frac{u^3}{R_{\rm D4}^{3/2}}h(u) & (M=2, N=3) \\ 0 & (\text{others}) \end{cases}. \tag{2.14}$$

We notice that the dependence of the DBI action on the noncommutativity parameter θ is canceled by the dilaton and the antisymmetric tensor field. The cancellation of the noncommutativity parameter dependence in the DBI action also takes place in the effective action of the probe D7 brane [16]. Adding the WZ term to the DBI action, we find the dependence on the noncommutativity parameter in the effective action of the D8 branes. Hereafter, the parameter $R_{\rm D4}$ is fixed to unity, $R_{\rm D4} = (\pi g_s N_c)^{1/3} l_s = 1$, for simplicity.

III. ELECTRIC FIELD

We investigate the response of the noncommutative deformation of holographic QCD at finite temperature to an external electric field E, by turning on an appropriate background value for the Abelian gauge field component of the unbroken $U(N_f)_V$ gauge field in the eight-brane world volume.

We make an ansatz,

$$2\pi\alpha' A_0 = \mu, \qquad 2\pi\alpha' A_1(t_E, u) = -iet_E + a_1(u), \tag{3.1}$$

where μ and e are constants.

A. Deconfinement phase

We first consider the deconfining background, which dominates at high temperature $T > 1/2\pi R$. The induced metric on the probe D8 brane is

$$ds^2 = u^{3/2}(f_T(u)dt_E^2 + (dx^1)^2 + h(u)\{(dx^2)^2 + (dx^3)^2\}) + [u^{3/2}(\tau'(u))^2 + u^{-3/2}f_T(u)^{-1}]du^2 + u^{1/2}d\Omega_4^2, \tag{3.2}$$

where the temperature T is related to the parameter u_T as $u_T = (16\pi^2/9)T^2$. The DBI action with the WZ term takes the form

$$S^{\rm D8} = S^{\rm D8}_{\rm DBI} + S^{\rm D8}_{\rm WZ} = \mathcal{N}\int d^4x du\left[u^4\sqrt{(f_T(u)\tau'(u)^2 + \frac{1}{u^3})\left(1 + \frac{e^2}{u^3 f_T(u)}\right) + \frac{f_T(u)(a_1'(u))^2}{u^3}} - 3\mu\theta^{3/2}u^3 h(u)a_1'(u)\right], \tag{3.3}$$

where $\mathcal{N}=\frac{2N_fN_c}{3(2\pi)^5(\alpha')^3}$ and the prime of a_1 denotes differentiation with respect to u. The baryon number current j_{eT} associated with the field a_1 is expressed as

$$j_{eT}=\frac{uf_T(u)a_1'(u)}{\sqrt{(f_T(u)\tau'(u)^2+\frac{1}{u^3})(1+\frac{e^2}{u^3f_T(u)})+\frac{f_T(u)(a_1'(u))^2}{u^3}}}-3\mu\theta^{3/2}u^3h(u). \tag{3.4}$$

The DBI action with the WZ term can be written in terms of the baryon number current as

$$S^{\mathrm{D8}}=\mathcal{N}\int d^4xduu^4\left\{1-\frac{3\mu\theta^{3/2}h(u)\tilde{j}_{eT}}{u^2f_T(u)}\right\}\times\sqrt{\frac{(f_T(u)\tau'(u)^2+\frac{1}{u^3})(f_T(u)-\frac{e^2}{u^3})}{(f_T(u)-\frac{\tilde{j}_{eT}^2}{u^2})}}, \tag{3.5}$$

where $\tilde{j}_{eT}=j_{eT}+3\mu\theta^{3/2}u^3h(u)$. Consider first a U-shaped embedding with a vanishing current $j_{eT}=0$. The corresponding action is given by

$$S^{\mathrm{D8}}=\mathcal{N}\int d^4xdu\frac{u^4}{f_T(u)}\sqrt{\left(f_T(u)\tau'(u)^2+\frac{1}{u^3}\right)\left(f_T(u)-\frac{e^2}{u^3}\right)(f_T(u)-9\mu^2\theta^3uh(u)^2)}. \tag{3.6}$$

The equation of motion for $\tau(u)$ is

$$\frac{d}{du}\left\{u^4\tau'(u)\sqrt{\frac{(f_T(u)-\frac{e^2}{u^3})(f_T(u)-9\mu^2\theta^3uh(u)^2)}{(f_T(u)(\tau'(u))^2+\frac{1}{u^3})}}\right\}=0. \tag{3.7}$$

$\tau'(u)$ satisfies the condition in the U-shaped embedding configuration: $\tau'\to\infty$ for $u\to u_0$. In the limit $u\to u_0$, we have the constant of the motion associated with $\tau(u)$ as

$$p_1=u_0^4\sqrt{\left(1-\frac{e^2}{u_0^3f_T(u_0)}\right)(f_T(u_0)-9\mu^2\theta^3u_0h(u_0)^2)}. \tag{3.8}$$

The solution of the equation of motion for $\tau(u)$ is

$$\tau'(u)=\frac{1}{u^{3/2}\sqrt{f_T(u)}}\left[\frac{u^8(1-\frac{e^2}{u^3f_T(u)})(f_T(u)-9\mu^2\theta^3uh(u)^2)}{u_0^8(1-\frac{e^2}{u_0^3f_T(u_0)})(f_T(u_0)-9\mu^2\theta^3u_0h(u_0)^2)}-1\right]^{-1/2}. \tag{3.9}$$

The reality conditions of the constant in (3.8) restricts the parameters e and θ as

$$e^2\le u_0^3-u_T^3,\qquad \theta^3\le K_{1-},\qquad \theta^3\ge K_{1+},$$
$$K_{1\pm}\equiv\frac{(9\mu^2-2u_0^2f_T(u_0))\pm3\mu\sqrt{9\mu^2-4u_0^2f_T(u_0)}}{2u_0^5f_T(u_0)}. \tag{3.10}$$

In the U-shaped embedding, the corresponding (on-shell) action is obtained by substituting (3.9) into (3.6):

$$S_{\mathrm{U}}^{\mathrm{D8}}=\mathcal{N}\int d^4xdu\frac{u^{5/2}}{f_T(u)}\sqrt{\left(f_T(u)-\frac{e^2}{u^3}\right)(f_T(u)-9\mu^2\theta^3uh(u)^2)}\times\left[1-\frac{u_0^8(1-\frac{e^2}{u_0^3f_T(u_0)})(f_T(u_0)-9\mu^2\theta^3uh(u_0)^2)}{u^8(1-\frac{e^2}{u^3f_T(u)})(f_T(u)-9\mu^2\theta^3uh(u)^2)}\right]^{-1/2}. \tag{3.11}$$

In the parallel embedding with $\tau'(u)=0$, the action becomes

$$S_{\parallel}^{\mathrm{D8}}=\mathcal{N}\int d^4xdu\frac{u^{5/2}}{f_T(u)}\left\{f_T(u)-\frac{3\mu\theta^{3/2}h(u)\tilde{j}_{eT}}{u^2}\right\}\sqrt{\frac{f_T(u)-\frac{e^2}{u^3}}{f_T(u)-\frac{\tilde{j}_{eT}^2}{u^5}}}. \tag{3.12}$$

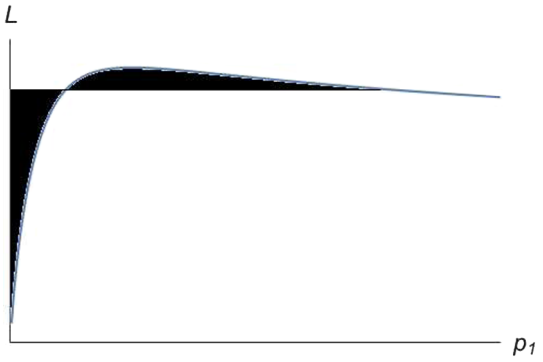

FIG. 3. Illustration of the Maxwell equal area construction.

The numerator of the fraction in the square root $f_T(u) - e^2/u^3$ is negative for $u^3 < u_T^3 + e^2$, which is always in the range of interaction. The only way to ensure a real action in this case is for the denominator in the same square root to become negative at the same u. This requires a nonvanishing current that is given by

$$j_{eT} = e(u_T^3 + e^2)^{1/3} - \frac{3\mu\theta^{3/2}(u_T^3 + e^2)}{1 + \theta^3(u_T^3 + e^2)}. \tag{3.13}$$

This current depends on the noncommutativity parameter θ. The parallel embedding therefore describes a chiral-symmetric conducting phase in the gauge theory, and the conductivity is given by

$$\sigma_e = \frac{(2\pi\alpha')^2\mathcal{N}}{V_4}\frac{j_{eT}}{e} = \frac{N_f N_c \lambda T^2}{27\pi}\left[(1+\tilde{e}^2)^{1/3} - \frac{3\tilde{\mu}\tilde{\theta}^{3/2}(1+\tilde{e}^2)}{\tilde{e}\{1+\tilde{\theta}^3(1+\tilde{e}^2)\}}\right], \tag{3.14}$$

where $\tilde{e} \equiv e/u_T^{3/2}$, $\tilde{\theta} \equiv u_T\theta$, and $\tilde{\mu} \equiv \mu/u_T$ are dimensionless parameters. The conductivity depends on the noncommutativity parameter and becomes the ordinary one in the limit of $\theta \to 0$ [23].

If the parallel embedding corresponds to the state of thermodynamic equilibrium, we can determine which of the two possible configurations is preferred by comparing the electric free energies of the two configurations [19]. However, the parallel embedding corresponds to the conducting phase, which is not in thermodynamic equilibrium. There is a steady-state current of quarks and antiquarks. Although the dissipated energy could be negligible, the kinetic energy of the current carriers should be taken into consideration.

To determine the transition temperature and transition electric field strength, we employ the Maxwell equal area construction method in the $L-p$ diagram. The dependence of p_1 on L can be determined numerically from (3.8) and (3.9) [with (2.9)] in the U-embedding configuration. The phase transition occurs when two regions enclosed by the $L-p$ curve and the horizontal L line (and L axis) are equal as shown by Fig. 3. We can determine the transition temperature T_c and the transition electric field strength e_c by seeking for various of T and e to satisfy the Maxwell equal area law and then construct the phase diagram in the (T, e) plane with fixed L and θ. The phase diagram at nonzero temperature, background electric field, and noncommutativity parameter in the deconfining phase is shown in Fig. 4. At zero electric field and zero noncommutativity parameter, the transition temperature reduces to the one of chiral symmetry breaking restoration [19].

The global behavior of the phase diagrams has not significantly changed even at finite noncommutativity parameter θ; that is, the transition temperature T_c decreases as the transition electric field strength e_c increases even at finite noncommutativity parameter θ. Although T_c at $e_c = 0$ is hardly changed, e_c at $T_c = 0$ increases with an increase in θ in the range of $0 \le \theta \le 0.50$. Both T_c at $e_c = 0$ and e_c at $T_c = 0$ decrease with decreasing θ in the range of $17.7 \le \theta$. As θ approaches infinity, both T_c and e_c turn back to them at the zero noncommutativity parameter. The reality condition is not satisfied in the range of $0.50 < \theta < 17.7$.

B. Confinement phase

We next consider the confining background, which dominates at low temperature $T < 1/2\pi R$. The induced metric on the probe D8 brane is

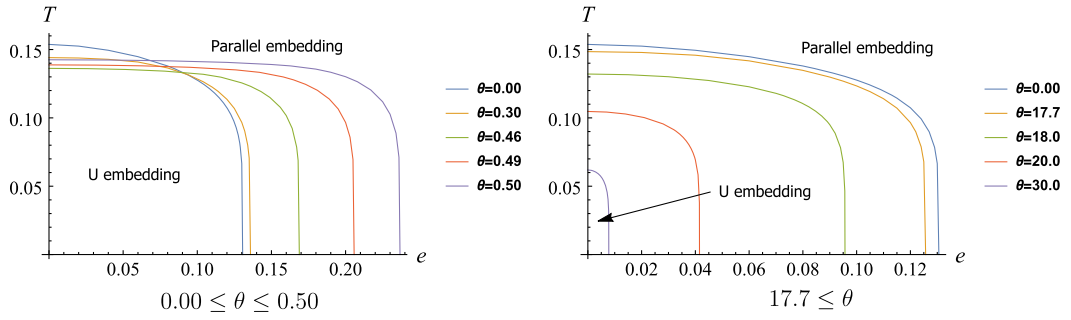

FIG. 4. Phase diagram at finite temperature and electric field in the deconfining background ($L = 1$, $\mu = 1$).

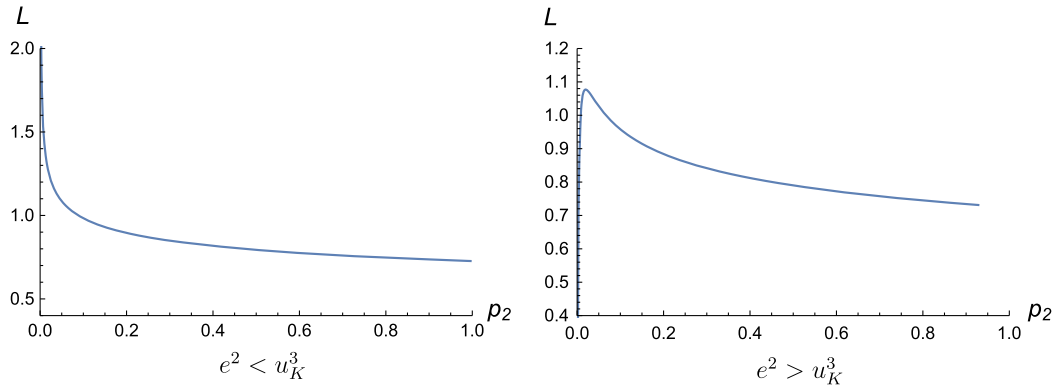

FIG. 5. Dependence of the asymptotic D8-$\bar{\text{D}}$8 distance L on p_2.

$$ds^2 = u^{3/2}(dt_E^2 + (dx^1)^2 + h(u)\{(dx^2)^2 + (dx^3)^2\}) + [u^{3/2} f_K(u)(\tau'(u))^2 + u^{-3/2} f_K(u)^{-1}]du^2 + u^{1/2} d\Omega_4^2. \tag{3.15}$$

The total effective action for the D8 branes is given by

$$\begin{aligned} S^{\mathrm{D8}} &= S^{\mathrm{D8}}_{\mathrm{DBI}} + S^{\mathrm{D8}}_{\mathrm{WZ}} \\ &= \mathcal{N} \int d^4x du \left[u^4 \sqrt{\left(f_K(u)\tau'(u)^2 + \frac{1}{u^3 f_K(u)} \right)\left(1 - \frac{e^2}{u^3}\right) + \frac{(a_1'(u))^2}{u^3}} - 3\mu\theta^{3/2} u^3 h(u) a_1'(u) \right] \\ &= \mathcal{N} \int d^4x du u^4 \left\{ 1 - \frac{3\mu\theta^{3/2} h(u)\tilde{j}_{eK}}{u^2} \right\} \sqrt{\frac{(f_K(u)\tau'(u)^2 + \frac{1}{u^3 f_K(u)})(1 - \frac{e^2}{u^3})}{(1 - \frac{\tilde{j}_{eK}^2}{u^2})}}, \end{aligned} \tag{3.16}$$

where $\tilde{j}_{eK} = j_{eK} + 3\mu\theta^{3/2} u^3 h(u)$ with

$$j_{eK} = \frac{u a_1'(u)}{\sqrt{(f_K(u)\tau'(u)^2 + \frac{1}{u^3 f_K(u)})(1 - \frac{e^2}{u^3}) + \frac{(a_1'(u))^2}{u^3}}} - 3\mu\theta^{3/2} u^3 h(u). \tag{3.17}$$

The solution of the equation of motion for $\tau(u)$ in the U embedding (with the vanishing j_{eK}) is given by

$$\tau'(u) = \frac{1}{u^{3/2} f_K(u)} \times \left[\frac{u^8 f_K(u)(1 - \frac{e^2}{u^3})(1 - 9\mu^2\theta^3 u h(u)^2)}{u_0^8 f_K(u_0)(1 - \frac{e^2}{u_0^3})(1 - 9\mu^2\theta^3 u_0 h(u_0)^2)} - 1 \right]^{-1/2}, \tag{3.18}$$

and the constant of motion for $\tau(u)$ is

$$p_2 = u_0^4 \sqrt{f_K(u_0)\left(1 - \frac{e^2}{u_0^3}\right)(1 - 9\mu^2\theta^3 u_0 h(u_0)^2)}. \tag{3.19}$$

In the same way as in the deconfinement phase, the reality conditions of the constant in (3.19) restrict the parameters e and θ,

$$e^2 \le u_0^3, \qquad \theta^3 \le K_{2-}, \qquad \theta^3 \ge K_{2+}, \qquad K_{2\pm} \equiv \frac{(9\mu^2 - 2u_0^2) \pm 3\mu\sqrt{9\mu^2 - 4u_0^2}}{2u_0^5}. \tag{3.20}$$

The asymptotic D8-$\overline{\text{D8}}$ distance L can be evaluate by using (3.18). The dependence of L on p_2 evaluated numerically from (3.18) and (3.19) is shown by Fig. 5. At no electric field, the only possible embedding in the confined phase is the U embedding, and L becomes a decreasing monotonic function of p_2. However, the behavior of L on p_2 can be modified under some external electric field. For $e^2 > u_K^3$, the asymptotic behavior of L becomes the same as in the deconfined phase. There is a threshold $e_{\mathrm{thr}} (> u_K^{3/2})$ that modifies the behavior of L on p_2, and the U embedding exists for $e < e_{\mathrm{thr}}$. For $e < e_{\mathrm{thr}}$, the corresponding (on-shell) action is given by

$$S^{\mathrm{D8}}_{\mathrm{U}} = \mathcal{N} \int d^4x du \frac{u^{5/2}}{\sqrt{f_T(u)}} \sqrt{\left(1 - \frac{e^2}{u^3}\right)(1 - 9\mu^2\theta^3 u h(u)^2)} \times \left[1 - \frac{u_0^8 f_K(u_0)(1 - \frac{e^2}{u_0^3})(1 - 9\mu^2\theta^3 u h(u_0)^2)}{u^8 f_K(u)(1 - \frac{e^2}{u^3})(1 - 9\mu^2\theta^3 u h(u)^2)} \right]^{-1/2}. \tag{3.21}$$

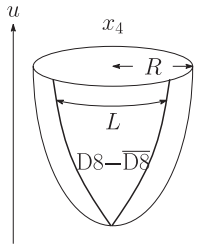

FIG. 6. The V embedding in the confining background.

The modification of the behavior of L suggests the existence of another kind of D8-$\overline{\text{D8}}$ embedding in the confining background. The D8 brane and $\overline{\text{D8}}$ brane are adjusted in parallel and are connected at $u = u_K$ in this embedding. We refer to this embedding as V-shaped embedding [23] (see Fig. 6).

In the V embedding, τ satisfies $\tau'(u) = 0$ except at $u = u_K$, and its action is given by

$$S_{\rm V}^{\rm D8} = \mathcal{N}\int d^4x du \frac{u^{5/2}}{\sqrt{f_K(u)}}\left\{1 - \frac{3\mu\theta^{3/2}h(u)\tilde{j}_{eT}}{u^2}\right\}\sqrt{\frac{1-\frac{e^2}{u^3}}{1-\frac{\tilde{j}_{eT}^2}{u^5}}}. \tag{3.22}$$

The reality condition for this action $S_{\rm V}^{\rm D8}$ in $e^2 > u_K^3$ implies the existence of the nonvanishing current in the following form:

$$j_{eK} = e^{5/3} - \frac{3\mu\theta^{3/2}e^2}{1+\theta^3 e^2}. \tag{3.23}$$

The V embedding is therefore a conductor with conductivity

$$\sigma_K = \frac{(2\pi\alpha')^2\mathcal{N}}{V_4}\frac{j_{eK}}{e} = \frac{N_f N_c \lambda}{48\pi^3}\left[e^{2/3} - \frac{3\mu\theta^{3/2}e}{1+\theta^3 e^2}\right]. \tag{3.24}$$

The conductivity also depends on the noncommutativity parameter as in the deconfinement phase and becomes the ordinary one in the limit of $\theta \to 0$ [23].

In the deconfinement phase, the current is produced due to the movement of quarks and antiquarks, namely, fundamental strings. In the confinement phase, the only charged objects are baryons. The current in the confinement phase can be regarded due to the movement of baryons and antibaryons, namely, D4 branes (and $\overline{\text{D4}}$ branes) wrapped on the S^4. It is thought that this stability of the cups singularity is provided by the balance of the forces caused by the D8 brane and the D4 branes pulling against each other. In accordance with this interpretation, we can evaluate the phase diagram in the (u_K, e) plane in the same way as the deconfining phase. The phase diagram in the (u_K, e) plane with fixed the D8-$\overline{\text{D8}}$-brane distance and θ in the confining phase is shown in Fig. 7.

The global behavior of the phase diagrams has also not significantly changed even at finite noncommutativity parameter θ in this situation; that is, the transition value of $u_K(=u_{Kc})$ increases as the transition electric field strength e_c increases. Whereas e_c at $T_c = 0$ with finite θ is bigger than that with $\theta = 0$ in the range of $0 \le \theta \le 0.50$, e_c at $T_c = 0$ with finite θ is smaller than that with $\theta = 0$ in the range of $17.7 \le \theta$. There is a tendency that e_c is modified by θ as u_{Kc} becomes smaller. We note that, even at finite noncommutativity parameter, e_c in the limit $u_{Kc} \to 0$ is the same as that in the deconfinement phase in the limit $T \to 0$ [23]. As θ approaches infinity, e_c at $T_c = 0$ turns back to them at zero noncommutativity parameter. The reality condition is not satisfied in the range of $0.50 < \theta < 17.7$ as in the deconfinement phase.

IV. MAGNETIC FIELD

We next investigate the response of the noncommutative deformation of the holographic QCD model at nonzero temperature to an external magnetic field B. We make an ansatz,

$$2\pi\alpha' A_0 = \mu, \qquad 2\pi\alpha' A_1(x_2, u) = -bx_2 + a_1(u), \tag{4.1}$$

where μ and b are constants. As was seen in the previous section, the noncommutativity also has the effect of varying the transition magnetic field strength b_c.

A. Deconfinement phase

Consider again the deconfining background, which dominates at high temperature $T > \frac{1}{2\pi R}$. The total action is given by

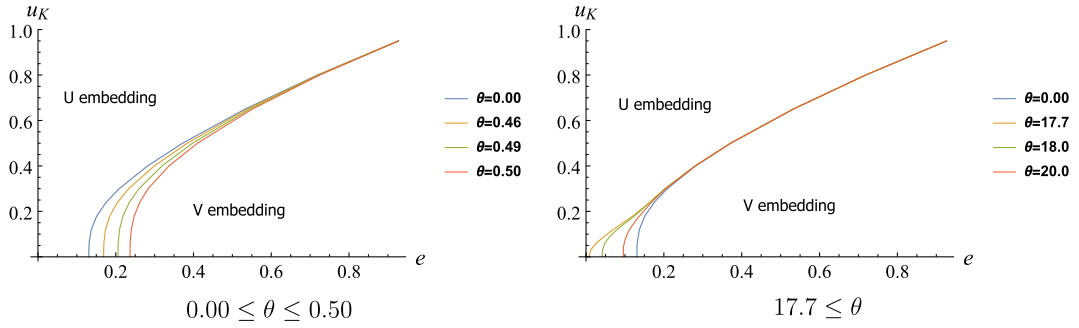

$0.00 \le \theta \le 0.50$ $17.7 \le \theta$

FIG. 7. Phase diagram at finite parameter u_K and the electric field in the confining background ($L = 1$, $\mu = 1$).

$$
\begin{aligned}
S^{\mathrm{D8}} &= S^{\mathrm{D8}}_{\mathrm{DBI}} + S^{\mathrm{D8}}_{\mathrm{WZ}} \\
&= \mathcal{N}\int d^4x du\left[u^4\sqrt{(f_T(u)\tau'\left(u\right)^2+\frac{1}{u^3}\Big)\Big(1+\frac{b^2}{u^3}\Big)+\frac{f_T(u)(a_1'(u))^2}{u^3}}-3\mu\theta^{3/2}u^3h(u)a_1'(u)\right] \\
&= \mathcal{N}\int d^4x du u^4\left\{1-\frac{3\mu\theta^{3/2}h(u)\tilde{j}_{bT}}{u^2 f_T(u)}\right\}\sqrt{\frac{(f_T(u)\tau'(u)^2+\frac{1}{u^3})(1+\frac{b^2}{u^3})}{(1-\frac{\tilde{j}_{bT}^2}{u^2 f_T(u)})}},
\end{aligned}
\tag{4.2}
$$

where $\tilde{j}_{bT} = j_{bT} + 3\mu\theta^{3/2}u^3h(u)$ with

$$
\begin{aligned}
j_{bT} = &\frac{u f_T(u)a_1'(u)}{\sqrt{(f_T(u)\tau'(u)^2+\frac{1}{u^3})(1+\frac{b^2}{u^3})+\frac{f_T(u)(a_1'(u))^2}{u^3}}} \\
&-3\mu\theta^{3/2}u^3h(u).
\end{aligned}
\tag{4.3}
$$

The solution of the equation of motion and the constant of motion for $\tau(u)$ in the U embedding (with the vanishing j_{bT}) are given, respectively, by

$$
\begin{aligned}
\tau'(u) = &\frac{1}{u^{3/2}\sqrt{f_T(u)}} \\
&\times\left[\frac{u^8(1+\frac{b^2}{u^3})(f_T(u)-9\mu^2\theta^3uh(u)^2)}{u_0^8(1+\frac{b^2}{u_0^3})(f_T(u_0)-9\mu^2\theta^3u_0h(u_0)^2)}-1\right]^{-1/2},
\end{aligned}
\tag{4.4}
$$

and

$$
p_3 = u_0^4\sqrt{f_T(u_0)\left(1+\frac{b^2}{u_0^3}\right)(f_T(u_0)-9\mu^2\theta^3u_0h(u_0)^2)}.
\tag{4.5}
$$

Although the reality conditions of the constant p_3 in (4.5) have no restriction for the parameter b, it has same restriction as (3.10) for the parameter θ.

In the U embedding, the corresponding (on-shell) action without j_{bT} is given by

$$
\begin{aligned}
S^{\mathrm{D8}}_{\mathrm{U}} = &\mathcal{N}\int d^4x du\frac{u^{5/2}}{\sqrt{f_T(u)}} \\
&\times\sqrt{\left(1+\frac{b^2}{u^3}\right)(f_T(u)-9\mu^2\theta^3uh(u)^2)} \\
&\times\left[1-\frac{u_0^8(1+\frac{b^2}{u_0^3f_T(u_0)})(f_T(u_0)-9\mu^2\theta^3uh(u_0)^2)}{u^8(1+\frac{b^2}{u^3f_T(u)})(f_T(u)-9\mu^2\theta^3uh(u)^2)}\right]^{-1/2}.
\end{aligned}
\tag{4.6}
$$

In the parallel embedding with $\tau'(u) = 0$, the action becomes

$$
\begin{aligned}
S^{\mathrm{D8}}_{\parallel} = &\mathcal{N}\int d^4x du\frac{u^{5/2}}{\sqrt{f_T(u)}}\left\{f_T(u)-\frac{3\mu\theta^{3/2}h(u)\tilde{j}_{bT}}{u^2}\right\} \\
&\times\sqrt{\frac{1+\frac{b^2}{u^3}}{f_T(u)-\frac{\tilde{j}_{bT}^2}{u^5}}}.
\end{aligned}
\tag{4.7}
$$

We can determine the transition temperature T_c and the transition magnetic field strength b_c by the Maxwell equal area law and construct the phase diagram in the (b, T) plane with fixed L and θ. The phase diagram at nonzero temperature, background magnetic field, and noncommutativity parameter in the deconfining phase is shown in Fig. 8.

The global behavior of the phase diagram has also not significantly changed even at finite noncommutativity

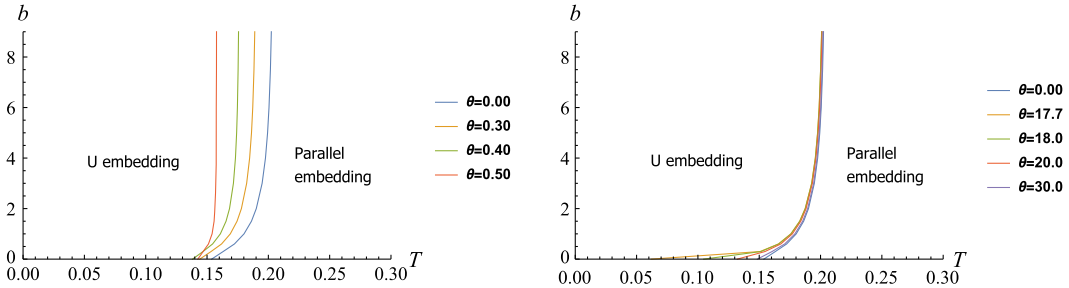

$0.00 \le \theta \le 0.50$ $\qquad$ $17.7 \le \theta$

FIG. 8. Phase diagram at finite temperature and magnetic field in the deconfining background ($L = 1$, $\mu = 1$).

parameter θ; that is, the transition temperature T_c increases as the transition magnetic field strength b_c increases even at finite noncommutativity parameter θ. Although T_c hardly changes at $b_c = 0$, it significantly changes in the large-b_c regime in the range of $0 \leq \theta \leq 0.50$. In contrast, although T_c significantly changes at $b_c = 0$, it hardly changes in the large-b_c regime in the range of $17.7 \leq \theta$. There is a tendency for T_c to decrease as θ increases in the range of $0 \leq \theta \leq 0.50$ and T_c to increase as θ increases in the range of $17.7 \leq \theta$. However, T_c at $b_c = 0$ with $\theta = 0.40$ becomes smaller than that at $b_c = 0$ with $\theta = 0.50$. As θ approaches infinity, both T_c and b_c turn back to them at zero noncommutativity parameter. The reality condition is not satisfied in the range of $0.50 < \theta < 17.7$.

B. Confinement phase

We next consider the confining background. In the U embedding, the solutions of the equation of motion for $\tau(u)$ and the constant of motion for $\tau(u)$ are given, respectively, by

$$\tau'(u) = \frac{1}{u^{3/2} f_K(u)} \times \left[\frac{u^8 f_K(u)(1+\frac{b^2}{u^3})(1-9\mu^2\theta^3 u h(u)^2)}{u_0^8 f_K(u_0)(1+\frac{b^2}{u_0^3})(1-9\mu^2\theta^3 u_0 h(u_0)^2)} - 1 \right]^{-1/2} \tag{4.8}$$

and

$$p_4 = u_0^4 \sqrt{f_K(u_0)\left(1+\frac{b^2}{u_0^3}\right)(1-9\mu^2\theta^3 u_0 h(u_0)^2)}. \tag{4.9}$$

The solution $\tau'(u)$ and the constant of motion p_4 are same as in (3.18) and in (3.19) with the substitution of $-e^2$ for b^2, respectively. Because of the difference in sign, the asymptotic D8-$\overline{\text{D8}}$ distance L is a decreasing monotonic function of p_4 for all values of b. It can be concluded that the only possible embedding in the confined phase is the U embedding. The on-shell action in the U embedding is given by

$$S_{\text{U}}^{\text{D8}} = \mathcal{N} \int d^4x du \frac{u^{5/2}}{\sqrt{f_T(u)}} \sqrt{\left(1+\frac{b^2}{u^3}\right)(1-9\mu^2\theta^3 u h(u)^2)} \times \left[1 - \frac{u_0^8 f_K(u_0)(1+\frac{b^2}{u_0^3})(1-9\mu^2\theta^3 u h(u_0)^2)}{u^8 f_K(u)(1+\frac{b^2}{u^3})(1-9\mu^2\theta^3 u h(u)^2)} \right]^{-1/2}. \tag{4.10}$$

V. CONCLUSIONS AND DISCUSSIONS

In this paper, we have constructed a noncommutative deformation of the holographic QCD (Sakai-Sugimoto) model at finite temperature in accordance with a prescription of Refs. [9–11,16] and have examined the response to external electric and magnetic fields regarding baryon number currents by this model. The noncommutative deformation of the gauge theory does not change the phase structure with respect to the baryon number current. There is also the conductor phase in addition to the insulator phase even in the noncommutative deformation of the confinement background at finite electric field [23]. However, the transition temperature T_c, the transition electric field e_c, and magnetic field b_c in the conductor-insulator phase transition depend on the noncommutativity parameter θ. Namely, the noncommutativity of space coordinates has an influence on the shape of the phase diagram for the conductor-insulator phase transition. It is known that the noncommutativity of space coordinates also has an influence on the shape of the phase diagram for the chiral symmetry breaking-chiral symmetry restoration within the framework of the noncommutative deformation of the holographic QCD model at finite temperature [22]. It can be regarded as an example that the noncommutativity of space coordinates reflects physical quantities [15,28].

The phase diagrams have shown that the transition temperature T_c, the transition electric field e_c, and magnetic field b_c shift to the commutative ones in the zero noncommutativity parameter limit. On the contrary, the phase diagrams have shown that T_c, e_c, and b_c also shift to the commutative ones in the infinite noncommutativity parameter limit. It can be easily seen that the nonvanishing currents j_{eT} and j_{eK} and the conductivities σ_T and σ_K reduce to the commutative ones in both the zero and infinite noncommutativity parameter limits. These properties are suggestive of a kind of Morita duality between irreducible modules over the noncommutative torus [6,16]. On the other hand, the allowed range of the noncommutativity parameter can be restricted by the reality condition of the constants of motion. It might be remarkable that the noncommutativity parameter is restricted by the physical conditions.

In the holographic QCD model, a chemical potential for baryon number corresponds to a nonzero asymptotic value of the electrostatic potential on the D8 branes [29–35]. In our model, a constant baryon chemical potential has been naively introduced. The dependence of T_c, e_c, and b_c on the baryon chemical potential should be considered in detailed procedures.

An alternative gravity dual of the confinement-deconfinement phase transition in the Sakai-Sugimoto model has been proposed in Refs. [36–38]. Reference [36] has argued that the gravity dual of the deconfinement transition is a Gregory-Laflamme transition into the T-dual type IIB supergravity, where the black D4-brane geometry is replaced by an localized D3-brane geometry. It would be interesting to study the properties of the baryon number current in this model.

The UV/IR mixing is well known as distinctive features of noncommutative field theories. The phenomenon of the UV/IR mixing appears to be the qualitative difference between ordinary and noncommutative field theory. The difference in the properties of the baryon number current between ordinary and noncommutative QCD might be related to the UV/IR mixing. We hope to discuss this subject in the future.

ACKNOWLEDGMENTS

We are grateful to C. Núñez for useful discussions and comments. One of us (T. N.) would like to thank members of the Physics Department at College of Engineering, Nihon University, for their encouragement. This work was supported in part by the overseas research fund of Nihon University.

[1] A. Connes, M. R. Douglas, and A. Schwarz, Noncommutative geometry and matrix theory: Compactification on tori, J. High Energy Phys. 02 (1998) 003.
[2] M. R. Douglas and C. Hull, D-branes and the noncommutative torus, J. High Energy Phys. 02 (1998) 008.
[3] F. Ardalan, H. Arfaei, and M. M. Sheikh-Jabbari, Noncommutative geometry from strings and branes, J. High Energy Phys. 02 (1999) 016.
[4] M. M. Sheikh-Jabbari, Super Yang-Mills theory on noncommutative torus from open strings interactions, Phys. Lett. B **450**, 119 (1999).
[5] N. Seiberg and E. Witten, String theory and noncommutative geometry, J. High Energy Phys. 09 (1999) 032.
[6] M. R. Douglas and N. A. Nekrasov, Noncommutative field theory, Rev. Mod. Phys. **73**, 977 (2001).
[7] R. J. Szabo, Quantum field theory on noncommutative spaces, Phys. Rep. **378**, 207 (2003).
[8] S. Minwalla, M. V. Raamsdonk, and N. Seiberg, Noncommutative perturbative dynamics, J. High Energy Phys. 02 (2000) 020.
[9] A. Hashimoto and N. Itzhaki, Noncommutative Yang-Mills and the AdS/CFT correspondence, Phys. Lett. B **465**, 142 (1999).
[10] J. M. Maldacena and J. G. Russo, Large N limit of noncommutative gauge theories, J. High Energy Phys. 09 (1999) 025.
[11] M. Alishahiha, Y. Oz, and M. M. Sheikh-Jabbari, Supergravity and large N noncommutative field theories, J. High Energy Phys. 11 (1999) 007.
[12] A. Dhar and Y. Kitazawa, Wilson loops in strongly coupled noncommutative gauge theories, Phys. Rev. D **63**, 125005 (2001).
[13] S. Lee and S.-j. Sin, Wilson loop and dimensional reduction in noncommutative gauge theories, Phys. Rev. D **64**, 086002 (2001).
[14] H. Takahashi, T. Nakajima, and K. Suzuki, D1/D5 system and Wilson loops in (non-)commutative gauge theories, Phys. Lett. B **546**, 273 (2002).
[15] T. Nakajima, K. Suzuki, and H. Takahashi, Glueball mass spectra for supergravity duals of noncommutative gauge theories, J. High Energy Phys. 01 (2006) 016.
[16] D. Arean, A. Paredes, and A. V. Ramallo, Adding flavor to the gravity dual of noncommutative gauge theories, J. High Energy Phys. 08 (2005) 017.
[17] T. Sakai and S. Sugimoto, Low energy hadron physics in holographic QCD, Prog. Theor. Phys. **113**, 843 (2005).
[18] T. Sakai and S. Sugimoto, More on a holographic dual of QCD, Prog. Theor. Phys. **114**, 1083 (2005).
[19] O. Aharony, J. Sonnenschein, and S. Yankielowicz, A holographic model of deconfinement and chiral symmetry restoration, Ann. Phys. (Amsterdam) **322**, 1420 (2007).
[20] A. Parnachev and D. A. Sahakyan, Chiral Phase Transition from String Theory, Phys. Rev. Lett. **97**, 111601 (2006).
[21] K. Peeters, J. Sonnenschein, and M. Zamaklar, Holographic melting and related properties of mesons in a quark gluon plasma, Phys. Rev. D **74**, 106008 (2006).
[22] T. Nakajima, Y. Ohtake, and K. Suzuki, Chiral symmetry restoration in holographic noncommutative QCD, J. High Energy Phys. 09 (2011) 054.
[23] O. Bergman, G. Lifschytz, and M. Lippert, Response of holographic QCD to electric and magnetic fields, J. High Energy Phys. 05 (2008) 007.
[24] C. V. Johnson and A. Kundu, External fields and chiral symmetry breaking in the Sakai-Sugimoto model, J. High Energy Phys. 12 (2008) 053.
[25] A. Karch and A. OfBannon, Metallic AdS/CFT, J. High Energy Phys. 09 (2007) 024.
[26] M. Ali-Akbari, Noncommutative holographic QCD and DC conductivity, J. High Energy Phys. 01 (2007) 072.
[27] Y. Seo, S.-j. Sin, and W.-s. Xu, Holographic model with a NS-NS field, Phys. Rev. D **80**, 106001 (2009).
[28] T. Nakajima, Y. Ohtake, and K. Suzuki, The spectrum of low spin mesons at finite temperature in holographic noncommutative QCD, Int. J. Mod. Phys. A **28**, 1350171 (2013).
[29] K. Y. Kim, S.-J. Sin, and I. Zahed, Dense hadronic matter in holographic QCD, J. Korean Phys. Soc. **63**, 1515 (2013).
[30] N. Horigome and Y. Tanii, Holographic chiral phase transition with chemical potential, J. High Energy Phys. 01 (2007) 072.
[31] A. Parnachev and D. A. Sahakyan, Photoemission with chemical potential from QCD gravity dual, Nucl. Phys. **B768**, 177 (2007).

[32] O. Bergman, G. Lifschytz, and M. Lippert, Holographic nuclear physics, J. High Energy Phys. 11 (2007) 056.
[33] D. Yamada, Sakai-Sugimoto model at high density, J. High Energy Phys. 10 (2008) 020.
[34] M. Rozali, H.-H. Shieh, M. Van Raamsdonk, and J. Wu, Cold nuclear matter in holographic QCD, J. High Energy Phys. 01 (2008) 053.
[35] K.-Y. Kim, S.-J. Sin, and I. Zahed, The chiral model of Sakai-Sugimoto at finite baryon density, J. High Energy Phys. 01 (2008) 002.
[36] G. Mandal and T. Morita, Gregory-Laflamme as the confinement/deconfinement transition in holographic QCD, J. High Energy Phys. 09 (**2011**) 073.
[37] G. Mandal and T. Morita, What is the gravity dual of the confinement/deconfinement transition in holographic QCD?, J. Phys. Conf. Ser. **343**, 012079 (2012).
[38] H. Isono, G. Mandal, and T. Morita, Thermodynamics of QCD from Sakai-Sugimoto Model, J. High Energy Phys. 12 (2015) 006.